

2006

Soft soil stabilisation with special reference to road and railway embankments

Buddhima Indraratna

University of Wollongong, buddhima_indraratna@uow.edu.au

C. Rujikiatkamjorn

University of Wollongong, cholacha@uow.edu.au

V. Wijeyakulasuriya

Department of Main Roads, Queensland

M. A. Shahin

University of Wollongong

D. Christie

RailCorp, Australia

Publication Details

This article was originally published as: Indraratna, B, Rujikiatkamjorn, C, Wijeyakulasuriya, V, Shahin, M, & Christie, D, Soft Soil Stabilisation with Special Reference to Railway Embankments, in D. Chan & K. T. Law (eds.), *Soft Soil Engineering: Proceedings of the 4th International Conference on Soft Soil Engineering, Vancouver, Canada, 4-6 October 2006*, Taylor & Francis, 35-56. Book information is available [here](#) from Taylor & Francis Books.

SOFT SOIL STABILISATION WITH SPECIAL REFERENCE TO ROAD AND RAILWAY EMBANKMENTS

Buddhima Indraratna, Professor of Civil Engineering, University of Wollongong, NSW 2522, Australia

Cholachat Rujikiatkamjorn, Research Fellow, University of Wollongong, NSW 2522, Australia

Vasantha Wijeyakulasuriya, Principal Geotechnical Engineer, Dept. of Main Roads, Brisbane, QLD, Australia

Mohamed A. Shahin, Research Fellow, University of Wollongong, NSW 2522, Australia

David Christie, Senior Geotechnical Advisor, RailCorp (Sydney), NSW, Australia

ABSTRACT

Much of Australian railway tracks traverse coastal areas containing soft soils and marine deposits. Pre-construction stabilization of soft formation soils by applying a surcharge load alone often takes too long. The installation of prefabricated vertical drains (PVDs) can reduce the preloading period significantly by decreasing the drainage path length, sometimes by a factor of 10 or more. The analytical solution based on actual radial soil permeability is proposed considering the variation of vacuum pressure, and the Cavity Expansion Theory is employed to predict the smear zone caused by the installation of mandrel driven vertical drains. The predicted smear zone and the effect of drain unsaturation are compared with data obtained from a large-scale radial consolidation tests and the results are explained. When a higher load is required to meet the desired rate of settlement and the cost of surcharge is also significant, the application of vacuum pressure with reduced surcharge loading can be used. In this method, an external negative load is applied to the soil surface in the form of vacuum pressure through a sealed membrane system. The applied vacuum pressure generates negative pore water pressure, resulting in an increase in effective stress and accelerated consolidation, also avoiding the need for a high surcharge embankment. The analytical and numerical analyses incorporating the authors' equivalent plane strain solution for both Darcian and non-Darcian flow are conducted to predict the excess pore pressures, lateral and vertical displacements and several selected case histories are analysed and presented. Cyclic loading of PVDs is also examined in the laboratory in a manner appropriate for railway environments. It is shown that short PVDs can dissipate excess pore pressure as fast as they are built up under repeated loading conditions. The research findings verify that the impact of smear and vacuum pressure can significantly affect soil consolidation, and these aspects need to be simulated properly in the selected numerical approach. Finally, the use of native vegetation to stabilise soft soils in railway environment is discussed with the aid of preliminary suction models developed on the basis of evapotranspiration mechanics applied to tree roots.

1. INTRODUCTION

Due to the rapid increase in population and associated development activities taking place, especially in the congested coastal areas, construction activities have become concentrated in low-lying marshy areas, which are comprised of highly compressible weak organic and peaty soils of varying thickness (Indraratna et al. 1992a). The entire coastal belt is dotted with very soft clays up to significant depths. These soft clay deposits have very low bearing capacity and excessive settlement characteristics, affecting major infrastructure including buildings, roads and rail tracks (Johnson 1970). Therefore, it is essential to stabilize the existing soft soils before commencing any construction activities in order to prevent differential settlements. Also in such low-lying areas it is necessary to raise the existing ground level to keep the surface above the groundwater table or flood level. A common practice to overcome these problems is to support the structure on special foundations, which could accommodate differential settlement to a greater degree, or to support them on pile foundations (Indraratna et al. 1992b, 2005a). In the case of a deep strong bearing stratum foundation, costs may become prohibitively high and not commensurate with the cost of the super

structure, for example in the case of rail tracks subject to cyclic loads (Broms 1987).

Preloading is the most successful ground improvement technique that can be used in low-lying areas. It involves loading of the ground surface to induce a greater part of the ultimate settlement that the ground is expected to experience after construction (Richart 1957; Indraratna and Redana 2000; Indraratna et al. 2005a). In order to control the development of excess pore pressures, this surcharge embankment is usually raised as a multi-stage exercise with rest periods provided between the loading stages (Jamiolkowski et al. 1983). Since most compressible soils are characterised by very low permeability and considerable thickness, the time needed for the required consolidation can be long, and also the surcharge load required may be significantly high (Indraratna et al. 1994). Currently this may not be possible with busy construction schedules. Installation of sand drains and geosynthetic vertical drains can reduce the preloading period significantly by decreasing the drainage path length in the radial direction, as the consolidation time is inversely proportional to the square of the length of the drainage path (Hansbo 1981; Indraratna and Redana 1998; Indraratna and Redana 2000). Due to the rapid initial consolidation, vertical

drains will increase the stiffness and bearing capacity of soft foundation clays (Bo et al., 2003).

Application of vacuum load can further accelerate the rate of settlement, generally compensating for the adverse effects of smear and well resistance (Indraratna et al. 2005b). Sand compaction piles provide significantly increased stiffness to soft compressible soils (Indraratna et al., 1997). Geosynthetic drains are usually composed of a plastic core (protected by fabric filter) with a longitudinal channel. The filter (sleeve) is made of synthetic or natural fibrous material with a high resistance to clogging. Vertical drains are applicable for moderately to highly compressible soils, which are usually normally consolidated or lightly over consolidated, and for stabilizing a deep layer of soil having a low permeability. The above remediation techniques allow coastal structures such as transport systems, embankments and tall buildings to be more stable under large static and cyclic loads.

In this paper, the effects of the compressibility indices, the variation of soil permeability and the magnitude of preloading are examined through the consolidation process. The smear zone prediction based on the Cavity Expansion Theory is discussed based on the large scale laboratory results. The equivalent (transformed) permeability coefficients for plane strain condition are incorporated in finite element codes, employing the modified Cam-clay theory. A case history is discussed and analysed, including the site of the New Bangkok International Airport (Thailand) and the predictions are compared with the available field data. The use of native vegetation for stabilising rail tracks is described with a selected case history, with the aim of achieving reduced track settlement.

2. CHARACTERISTICS OF VERTICAL DRAINS SYSTEM

2.1 Purpose and Application of Vertical Drains

Various types of vertical drains including sand drains, sand compaction piles, prefabricated vertical drains (geosynthetic) and gravel piles have been commonly used in the past. Apart from increasing cost of sand quarrying in some countries and conventional sand drains that can be damaged from lateral ground movement, the flexible prefabricated vertical drains (PVD) systems with relatively more rapid installation have replaced the original sand drains and gravel piles. The most common band shaped drains have dimensions of 100mm × 4mm. For design purposes, the rectangular (width- a , thickness- b) section must be converted to an equivalent circle (diameter, d_w) because, the conventional theory of radial consolidation assumes circular drains(Fig. 1).

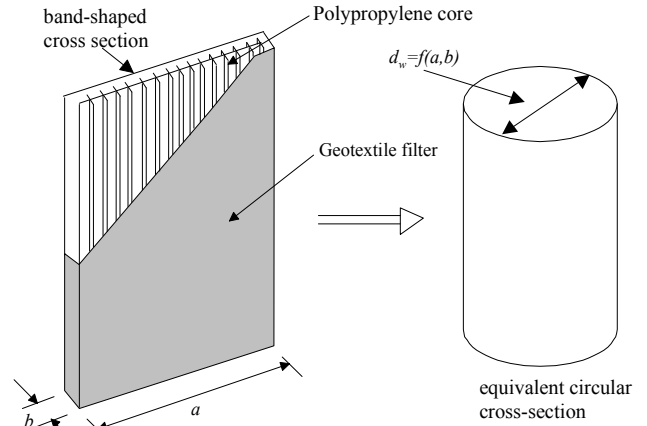


Figure 1 Conceptual illustration of band-shaped PVD and equivalent diameter of drain well (Indraratna et al., 2005f)

The following typical equation is used to determine the equivalent drain diameter:

$$d_w = 2(a + b)/\pi \quad (\text{Hansbo, 1979}) \quad (1)$$

Atkinson and Eldred (1981) proposed that a reduction factor of $\pi/4$ should be applied to Eq. 1 to take account of the corner effect where the flow lines rapidly converge. From the finite element studies, Rixner et al. (1986) proposed that:

$$d_w = (a + b)/2 \quad (2)$$

Pradhan et al. (1993) suggested that the equivalent diameter of band-shaped drains should be estimated by considering the flow net around the soil cylinder of diameter d_e (Fig. 2). The mean square distance of their flow net is calculated as:

$$s^2 = \frac{1}{4}d_e^2 + \frac{1}{12}a^2 - \frac{2a}{\pi^2}d_e \quad (3)$$

$$\text{Then, } d_w = d_e - 2\sqrt{\left(\frac{-2}{s}\right)} + b \quad (4)$$

More recently, Long and Covo (1994) found that the equivalent diameter d_w could be computed using an electrical analogue field plotter:

$$d_w = 0.5a + 0.7b \quad (5)$$

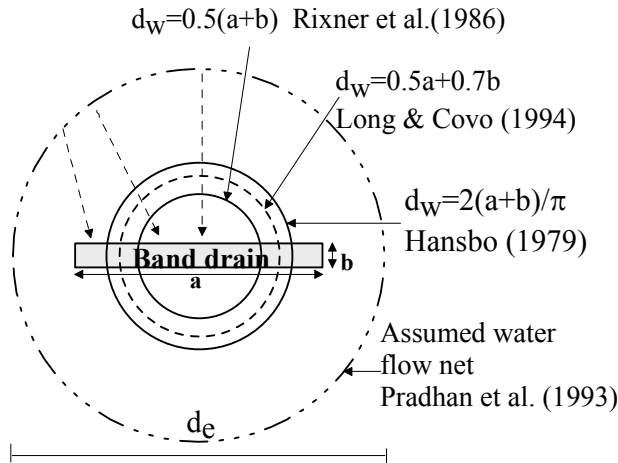


Figure 2 Assessment of equivalent diameter of band shaped vertical drains (Indraratna et al., 2005f)

The discharge capacity is one of the most important parameter that controls the performance of prefabricated vertical drains. The discharge capacity depends primarily on the following factors (Fig. 3): (i) the area of the drain; (ii) the effect of lateral earth pressure; (iii) possible folding, bending and crimping of the drain and (iv) infiltration of fine particles into the drain filter.

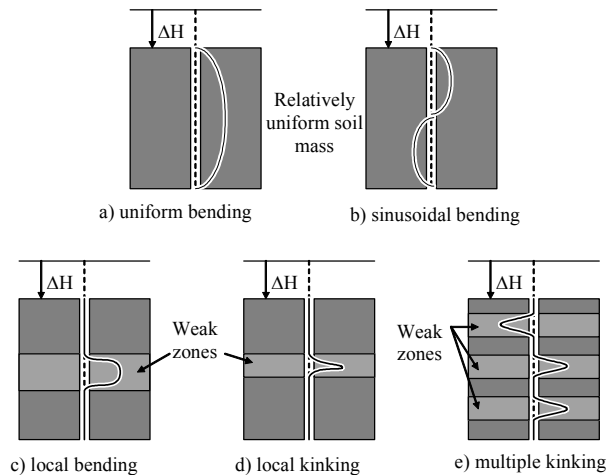


Figure 3 PVD Deformation modes (after Holtz et al. 1991)

In practice, static and dynamic methods can be used to install vertical drains. Static procedure is preferred for driving the mandrel into the ground, whereas the dynamic methods seem to create a greater disturbance to the surrounding soil during installation (e.g. drop hammer impact or vibrating hammer). A typical installation rig is shown in Fig. 4. The degree of disturbance during installation depends on several factors such as the soil types, mandrel size, mandrel shape and soil macrofabric. The sand blanket system is employed to expel water

away from the drains and to provide a sound-working mat for vertical drain rigs.

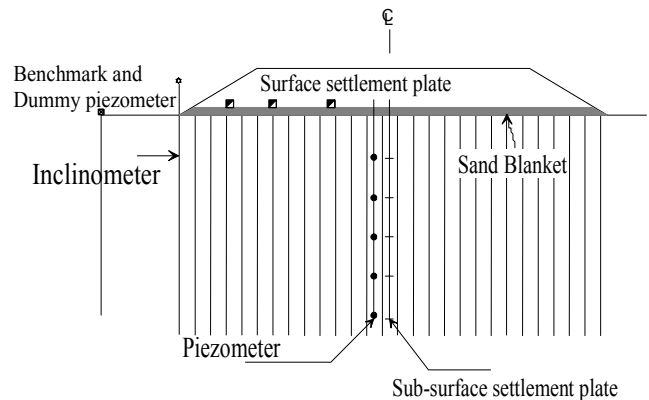


Figure 4 System of PVDs with sand blanket and surcharge preloading (Indraratna et al. 2005d)

Before installing the vertical drains, general site preparations including the removal of vegetation and surficial soil, establishing site grading and placing a compact sand blanket are required.

Field instrumentation for monitoring and evaluating the performance of embankments is vital to examine and control the geotechnical problems. Based on the construction stages, field instrumentation can be separated into two categories (Bo et al., 2003). The first category is employed to prevent sudden failures during construction (e.g. settlement plates, inclinometers and piezometers), whereas the second group is used to record changes in the rate of settlement and excess pore pressure during loading stages (e.g. multilevel settlement gauges and piezometers).

2.2 Principles of PVD with Vacuum Preloading

The vacuum preloading method was originally introduced in Sweden by Kjellman (1952) for cardboard wick drains. It has been used extensively to accelerate the consolidation process for improving soft ground, such as Philadelphia International Airport, USA and Tianjin port, China (Holtan, 1965 and Yan and Chu, 2003). When a higher surcharge load is required to meet the expected settlement and this cost becomes substantial, a combined vacuum and fill surcharge can be employed. In very soft clay area, where a high surcharge embankment cannot be constructed without affecting stability, the vacuum application is preferable. Recently, the PVD system has also been employed to distribute vacuum pressure to deep subsoil layer, thereby increasing the consolidation rate of reclaimed land from the sea (e.g. Indraratna et al. 2005d, Chu et al. 2000). The mechanism of the vacuum preloading can be described by the spring analogy provided by Chu and Yan (2005) (Fig. 5). The effective stress increases through vacuum load while the total stress remains constant.

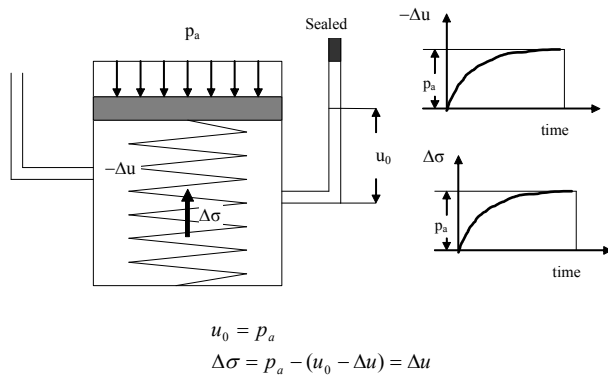


Figure 5 Spring analogy of vacuum consolidation process (adopted from Chu and Yan, 2005)

For vacuum-assisted preloading, the installation of some horizontal drains in the transverse and longitudinal directions is compulsory after installing the sand blanket. Subsequently, these drains can be connected to the edge of a peripheral Bentonite slurry trench, which is normally sealed by an impervious membrane (Fig. 6). The trenches can then be filled with water to improve sealing between the membrane and Bentonite slurry. The vacuum pumps are connected to the prefabricated discharge system extending from the trenches, and the suction head generated by the pump accelerates dissipation of excess pore water pressure in the soil towards the drains and the surface.

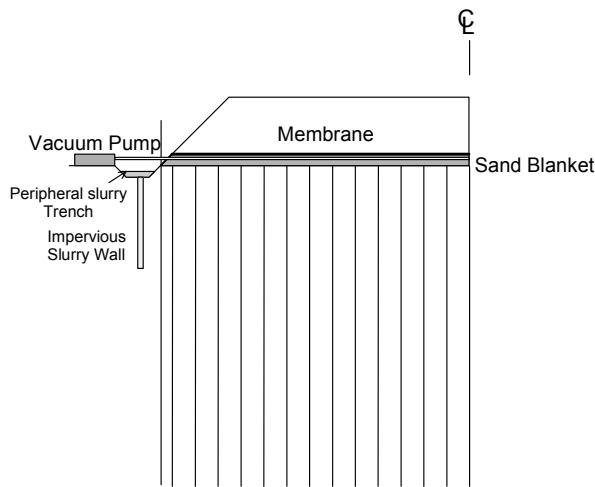


Figure 6 Vacuum-assisted preloading system (Indraratna et al. 2005d)

The characteristics of vacuum preloading in comparison with conventional preloading are as follows (Qian et al., 1992):

- The effective stress related to suction pressure increases equiaxially, and the corresponding lateral movement is compressive. Consequently, the risk of shear failure can be minimized even at a higher rate of embankment construction. However, the 'inward'

movement to embankment toe should be carefully monitored.

- The vacuum head can be distributed to a greater depth of the subsoil using the PVD system.
- The extent of surcharge fill can be decreased to achieve the same amount of settlement, depending on the efficiency of the vacuum system in the field (i.e., air leaks).
- Since the surcharge height can be reduced, the maximum excess pore pressure generated by vacuum preloading is less than the conventional surcharge method (Fig. 7).
- With vacuum pressure, the inevitable unsaturated condition at the soil-drain interface may be improved, resulting in an increased rate of consolidation.

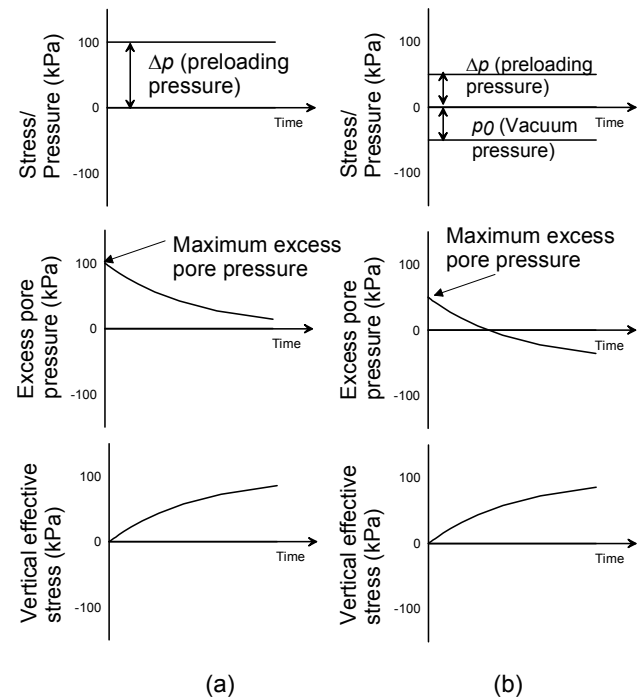


Figure 7 Consolidation process: (a) conventional loading (b) idealised vacuum preloading (Indraratna et al. 2005d)

2.3 Field Observation of Retarded Pore Pressure Dissipation

It has been observed in some case studies that in spite of PVDs, excess pore water pressures sometimes do not dissipate as expected. This is often attributed to filter clogging, extreme reduction of the lateral permeability of soil, damage to piezometer tips etc. However, recent numerical analysis suggests that very high lateral strains and corresponding stress redistributions (e.g. substantial heave at the embankment toe) can also contribute to retarded rate of pore pressure dissipation. Some examples are shown in Figs. 8 and 9.

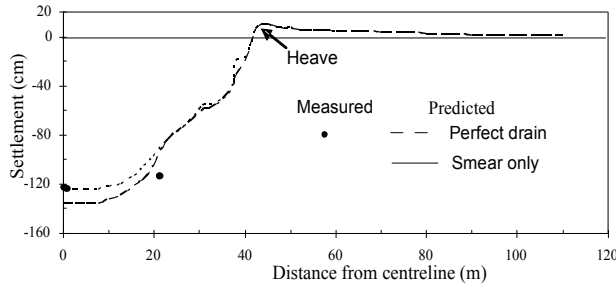


Figure 8 Surface settlement profile after 400 days (Indraratna & Redana, 2000; Indraratna & Chu, 2005)

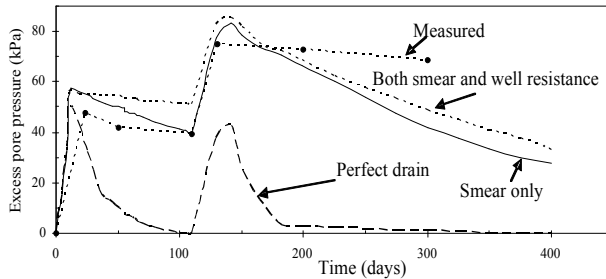


Figure 9 Excess pore water pressure variation at piezometer location, P6 (after Indraratna & Redana, 2000; Indraratna & Chu, 2005)

3. THEORY OF RADIAL CONSOLIDATION

3.1 Axisymmetric unit cell analysis

Linear Darcian flow:

Conventional radial consolidation theory (including smear and well resistance) has been commonly employed to predict the behaviour of vertical drains in soft clay. Its mathematical formulation is based on the small strain theory, and for a given stress range, a constant volume compressibility (m_v) and a constant coefficient of lateral permeability (k_h) are assumed (Barron 1948, Hansbo 1981). However, the value of m_v varies along the consolidation curve over a wide range of applied pressure (Δp). In the same manner, k_h also changes with the void ratio (e). Indraratna et al. (2005c) have replaced m_v with the compressibility indices (C_c and C_r), which define the slopes of the e - $\log \sigma$ relationship. Moreover, the variation of horizontal permeability coefficient (k_h) with void ratio (e) during consolidation is represented by the e - $\log k_h$ relationship that has a slope of C_k .

The main assumptions are given below (Indraratna et al. 2005c):

(1) Homogenous soil is fully saturated whereby Darcy's law is adopted. At the external periphery of the unit cell, flow is not allowed to occur (Fig. 10). For relatively long vertical drains, only radial (horizontal) flow is allowed (i.e. no vertical flow).

(2) Soil strain is uniform at the upper boundary of the unit cell (i.e. no differential settlement in a unit cell). The small strain theory is valid.

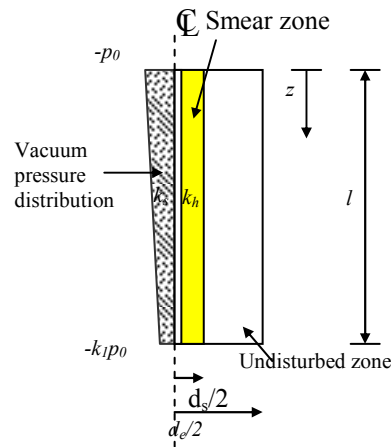


Figure 10 Cylindrical unit cell with linear vacuum pressure distribution (modified after Indraratna et al., 2005d)

(3) The relationship between the average void ratio and the logarithm of average effective stress in the normally consolidated range (Fig. 11) can be expressed by: $\bar{e} = e_0 - C_c \log(\sigma' / \sigma'_i)$. If the current vertical effective stress (σ') is less than p'_c , then for this overconsolidated range, the recompression index (C_r) is used rather than C_c .

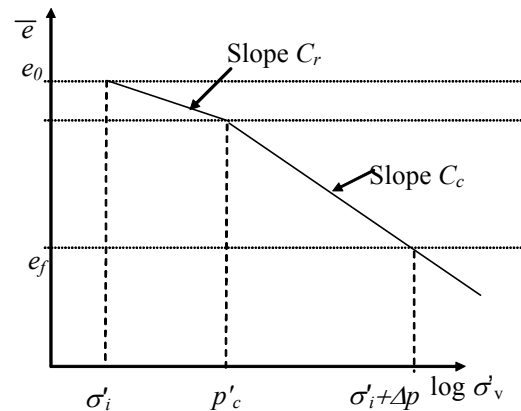


Figure 11 Soil compression curve (after Indraratna et al., 2005c)

(4) For radial drainage, the horizontal permeability of soil decreases with the average void ratio (Fig. 12). The relationship between these two parameters is given by Tavenas et al. (1983): $\bar{e} = e_0 + C_k \log(k_h / k_{hi})$. The permeability index (C_k) is generally considered to be independent of stress history (p'_c) as explained by Nagaraj et al. (1994).

(5) According to Indraratna et al. (2004), the vacuum pressure distribution along the drain boundary is considered to vary linearly from $-p_0$ at top of the drain to $-k_1 p_0$ at the bottom of the drain, where k_1 is a ratio between vacuum pressure at the bottom and the top of the drain (Fig. 10)

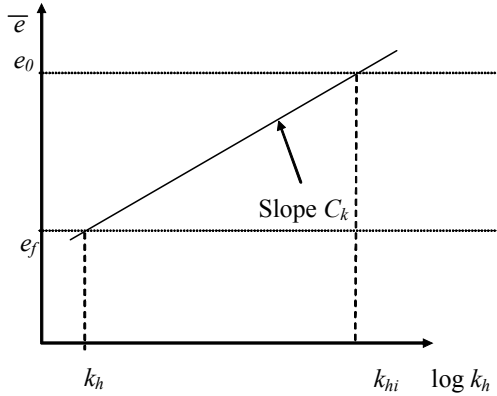


Figure 12 Semi-log permeability-void ratio (after Indraratna et al., 2005c)

The dissipation rate of average excess pore pressure ratio ($R_u = \bar{u}_t / \Delta p$) at any time factor (T_h) can be expressed as:

$$R_u = \left(1 + \frac{p_0(1+k_1)}{\Delta p}\right) \exp\left(\frac{-8T_h^*}{\mu}\right) - \frac{p_0(1+k_1)}{\Delta p} \quad (6)$$

In the above expression,

$$T_h^* = P_{av} T_h \quad (7)$$

$$P_{av} = 0.5 \left[1 + \left(1 + \Delta p / \sigma'_i + p_0(1+k_1) / 2\sigma'_i\right)^{1-C_c/C_k} \right] \quad (8)$$

$$T_h = c_h t / d_e^2 \quad (9)$$

$$\mu = \ln \frac{n}{s} + \frac{k_h}{k'_h} \ln s - 0.75 \quad (10)$$

where, μ = a group of parameters representing the geometry of the vertical drain system and smear effect, $n = d_e/d_w$, $s = d_s/d_w$, d_e = equivalent diameter of cylinder of soil around drain, d_s = diameter of smear zone and d_w = diameter of drain well, k_h = average horizontal permeability in the undisturbed zone (m/s), and k'_h = average horizontal permeability in the smear zone (m/s). Δp = preloading pressure, T_h is the dimensionless time factor for consolidation due to radial drainage.

Since the relationship between effective stress and strain is non-linear, the average degree of consolidation can be described either based on excess pore pressure (stress) (U_p) or based on strain (U_s). U_p indicates the rate of dissipation of excess pore pressure whereas U_p shows the rate of development of the surface settlement. Normally, $U_p \neq U_s$ except when the effective stress and strain is a linear relationship, which is in accordance with Terzaghi's one-dimensional theory. Therefore, the average degree of consolidation based on excess pore pressure can be obtained as follows:

$$U_p = 1 - R_u \quad (11)$$

The average degree of consolidation based on settlement (strain) is defined by:

$$U_s = \frac{\rho}{\rho_\infty} \quad (12)$$

The associated settlements (ρ) are then evaluated by the following equations:

$$\rho = \frac{HC_r}{1+e_0} \log\left(\frac{\sigma'}{\sigma'_i}\right), \quad \sigma'_i \leq \sigma' \leq p'_c \quad (13a)$$

$$\rho = \frac{H}{1+e_0} \left[C_r \log\left(\frac{p'_c}{\sigma'_i}\right) + C_c \log\left(\frac{\sigma'}{p'_c}\right) \right], \quad p'_c \leq \sigma' \leq \sigma'_i + \Delta p \quad (13b)$$

$$\rho = \frac{HC_c}{1+e_0} \log\left(\frac{\sigma'}{\sigma'_i}\right) \quad \text{for normally consolidated clay} \quad (13c)$$

It is noted that ρ_∞ can be obtained by substituting $\sigma' = \sigma'_i + \Delta p$ into the above equations. In the above equations, ρ = settlement at a given time, ρ_c = total primary consolidation settlement, σ'_i = effective in-situ stress, σ' = effective stress, C_c = compression index, C_r = recompression index and H = compressible soil thickness.

Depending on the location of the initial and final effective stresses with respect to the normally consolidated and overconsolidated domains, the following is a summary of the relevant computational steps.

(1) If both the initial and final effective stresses are in the normally consolidated range, Equations (6) and (11) are employed to calculate U_p , whereas Equations (12) and (13c) are used to compute U_s .

(2) If both the initial and final effective stresses are in the overconsolidated range, Equations (6) and (11) are employed to calculate U_p , and Equations (12) and (13a) are used to determine U_s .

(3) If the initial effective stress falls on the overconsolidated domain and the final effective stress is on the normally consolidated domain, then Equations (6) and (11) are employed to calculate U_p , Equations (12) (13a) and (13b) are employed to calculate U_s .

When the value of C_o/C_k approaches unity and p_o becomes zero, the authors' solution converges to the conventional solution proposed by Hansbo (1981):

$$R_u = \exp(-8T_h/\mu) \quad (14)$$

Non-Darcian flow:

Hansbo (1997) stated that at small hydraulic gradients, conventional linear Darcy's law may be replaced by a non-Darcian flow condition defined by an exponential relationship. Based on non-Darcian flow, Hansbo (1997) modified the classical axisymmetric solutions. The pore water flow velocity, v caused by a hydraulic gradient, i might deviate from the original Darcy's law $v = k i$, where under a certain gradient i_o below which no flow occurs. Then the rate of flow is given by: $v = k (i - i_o)$, hence, the following relations have been proposed:

$$v = \kappa i^n \text{ for } i \leq i_1 \quad (15)$$

$$v = k(i - i_o) \text{ for } i \geq i_1 \quad (16)$$

$$\text{where } i_1 = \frac{i_o n}{(n-1)} \text{ and } \kappa = (n^{-1} i_1^{1-n}) k \quad (17)$$

In order to study the non-Darcian effects, Hansbo (1979, 1997) proposed an alternative consolidation equation. The time required to reach a certain average degree of consolidation including smear effect is given by:

$$t = \frac{\alpha D^2}{\lambda} \left(\frac{D \gamma_w}{u_o} \right)^{n-1} \left(\frac{1}{(1 - \bar{U}_h)^{n-1}} - 1 \right) \quad (18a)$$

where the coefficient of consolidation $\lambda = \frac{\kappa_h M}{\gamma_w}$, $M=1/m_v$

is the oedometer modulus, D is the diameter of the drain influence zone, d_s is the diameter of smear zone, $n=D/d_w$ where d_w is the drain diameter, u_o is the initial average

excess pore water pressure, and α is $\frac{n^{2n} \beta^n}{4(n-1)^{n+1}}$ where,

$$\beta = \frac{1}{3n-1} - \frac{n-1}{n(3n-1)(5n-1)} - \frac{(n-1)^2}{2n^2(5n-1)(7n-1)} + \frac{1}{2n} \left[\left(\frac{\kappa_h}{\kappa_s} - 1 \right) \left(\frac{D}{d_s} \right)^{-(1-(1/n))} - \frac{\kappa_h}{\kappa_s} \left(\frac{D}{d_w} \right)^{-(1-(1/n))} \right] \quad (18b)$$

When $n \rightarrow 1$ Eq. (18) gives the same result as the average degree of consolidation represented by Eq. (9), provided

that well resistance is neglected and assuming $\lambda = c_h$ and $\kappa_p/\kappa_s = k_p/k_s$.

3.2 Equivalent Plane Strain Approach for Multi-drain Analysis

For multi-drain simulation, the plane strain finite element analysis can be readily adapted to most field situations (Hansbo 1981; Indraratna and Redana 1997; Indraratna and Redana 2000). Nevertheless, realistic field predictions require the axisymmetric properties to be converted to an *equivalent* 2D plane strain condition, especially with regard to the permeability coefficients and drain geometry (Indraratna and Redana 1997). The plane strain analysis can also accommodate vacuum preloading in conjunction with vertical drains (e.g. Gabr and Szabo 1997). Mohamedel Hassan and Shang (2002) discussed the application of vacuum pressure and its benefits, but without any vertical drains. Subsequently, Indraratna et al. (2005b) proposed the equivalent plane strain approach for the simulation of vacuum pressure for the vertical drain system.

Darcian Flow:

Indraratna and Redana (1997, 1998, 2000) and Indraratna et al. (2005b) converted the vertical drain system shown in Fig. 13 into an equivalent parallel drain wall by adjusting the coefficient of permeability of the soil, and by assuming the plane strain cell (a width of $2B$). The half width of the drain b_w and half width of the smear zone b_s may be kept the same as their axisymmetric radii r_w and r_s , respectively, which suggests $b_w = r_w$ and $b_s = r_s$.

Indraratna et al. (2005b) proposed the average degree of consolidation in plane strain condition by:

$$\frac{\bar{u}}{u_o} = \left(1 + \frac{P_{0p}}{u_o} \frac{(1+k_1)}{2} \right) \exp \left(-\frac{8T_{hp}}{\mu_p} \right) - \frac{P_{0p}}{u_o} \frac{(1+k_1)}{2} \quad (19a)$$

and

$$\mu_p = \left[\alpha + (\beta) \frac{k_{hp}}{k'_{hp}} \right] \quad (19b)$$

where, \bar{u}_o = initial excess pore pressure, \bar{u} = pore pressure at time t (average values) and T_{hp} = time factor in plane strain, k_{hp} and k'_{hp} are the undisturbed horizontal and the corresponding smear zone equivalent permeabilities, respectively. The geometric parameters α and β , are given by:

$$\alpha = \frac{2}{3} - \frac{2b_s}{B} \left(1 - \frac{b_s}{B} + \frac{b_s^2}{3B^2} \right) \quad (20a)$$

$$\beta = \frac{1}{B^2} (b_s - b_w)^2 + \frac{b_s}{3B^3} (3b_w^2 - b_s^2) \quad (20b)$$

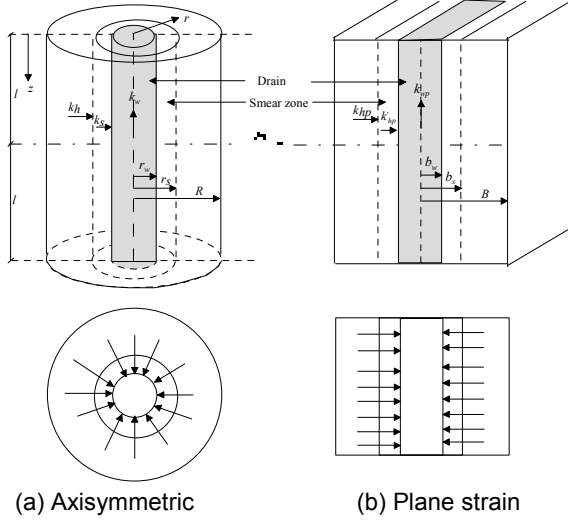


Figure 13 Conversion of an axisymmetric unit cell into plane strain condition (after Indraratna and Redana, 2000)

At a given effective stress level and at each time step, the average degree of consolidation for both axisymmetric (\bar{U}_p) and equivalent plane strain ($\bar{U}_{p,pl}$) conditions are made equal, hence:

$$\bar{U}_p = \bar{U}_{p,pl} \quad (21)$$

Combining Equations (14) and (17) with equation (14) of original Hansbo theory (Hansbo, 1981), the time factor ratio can be represented by the following equation:

$$\frac{T_{hp}}{T_h} = \frac{k_{hp}}{k_h} \frac{R^2}{B^2} = \frac{\mu_p}{\mu} \quad (22)$$

Making the magnitudes of R and B to be the same, Indraratna and Redana (2000) presented a relationship between k_{hp} and k_{hp}' . The influence of smear effect can be modelled by the ratio of the smear zone permeability to the undisturbed permeability, as follows:

$$\frac{k_{hp}'}{k_{hp}} = \frac{\beta}{\frac{k_{hp}}{k_h} \left[\ln\left(\frac{n}{s}\right) + \left(\frac{k_h}{k_h'}\right) \ln(s) - 0.75 \right] - \alpha} \quad (23)$$

If smear and well resistance effects are ignored in the above expression, then the simplified ratio of plane strain to axisymmetric permeability is readily obtained, as also proposed earlier by Hird et al. (1992), as follows:

$$\frac{k_{hp}}{k_h} = \frac{0.67}{\ln(n) - 0.75} \quad (24)$$

For vacuum preloading, the equivalent vacuum pressure in plane strain and axisymmetric are the same.

Non-Darcian Flow:

Sathananthan and Indraratna (2005) determined the solution for equivalent plane strain under non-Darcian flow. The converted permeability relationship is given by:

$$\kappa_{hp} = 2\kappa_h \left(\frac{n-1}{2n^2} \frac{\beta_p}{\beta} \right)^n \quad (25)$$

Ignoring the smear effect in Eq. (25), the equivalent plane strain permeability in the undisturbed zone is now obtained as:

$$\frac{\kappa_{hp}}{\kappa_h} = \frac{\lambda_{hp}}{\lambda} = 2 \left(\frac{f_p \left(n, \frac{b_w}{B} \right)}{2f \left(n, \frac{r_w}{R} \right)} \right)^n \quad (26a)$$

4. SMEAR ZONE DETERMINATION

Sathananthan (2005) made an attempt to estimate the extent of "smear zone", caused by mandrel installation using the Cylindrical Cavity Expansion theory incorporating the modified Cam-clay model (MCC) as explained elsewhere by Collins & Yu (1996) and Cao et al. (2001). Only a summary is given below. For soil obeying the MCC model, the yielding criterion is:

$$\eta = M \sqrt{\left(\frac{p_c'}{p'} \right) - 1} \quad (27)$$

where, p_c' : the stress representing the reference size of yield locus, p' = mean effective stress, M = slope of the critical state line and η = stress ratio. Stress ratio at any point can be determined as follows:

$$\ln \left(1 - \frac{(a^2 - a_0^2)}{r^2} \right) = - \frac{2(1+\nu)}{3\sqrt{3}(1-2\nu)} \frac{\kappa}{\nu} \eta - 2\sqrt{3} \frac{\kappa\Lambda}{\nu M} f(M, \eta, OCR) \quad (28)$$

where,

$$f(M, \eta, OCR) = \frac{1}{2} \ln \left[\frac{(M+\eta)(1-\sqrt{OCR-1})}{(M-\eta)(1+\sqrt{OCR-1})} \right] - \tan^{-1} \left(\frac{\eta}{M} \right) + \tan^{-1} \left(\sqrt{OCR-1} \right) \quad (29)$$

where, a = radius of the cavity, a_0 = initial radius of the cavity, ν = Poisson's ratio, κ = slope of the overconsolidation line, ν = specific volume, OCR = over consolidation ratio and $\Lambda = 1 - \kappa/\lambda$ (λ is the slope of the

normal consolidation line). Finally, the corresponding mean effective stress, in terms of deviatoric stress, total stress and excess pore pressure, can be expressed by the following expressions:

$$p' = p_0' \left[\frac{OCR}{1 + (\eta/M)^2} \right]^\Lambda \quad (30)$$

$$q = \eta p' \quad (31)$$

$$p = \sigma_{rp} - \frac{q}{\sqrt{3}} + \frac{2}{\sqrt{3}} \int_r^{r_p} \frac{q}{r} dr \quad (32)$$

Employing Equations (30)-(32), the excess pore pressure due to mandrel driving (Δu) can be determined by:

$$\Delta u = (p - p_0) - (p' - p_0') \quad (33)$$

where, p_0 = initial total mean stress. The extent of the smear zone can be suggested as the region in which the excess pore pressure tends to exceed the initial overburden pressure (σ'_{v0}) (Fig. 14). This is because, in the region surrounding the drains ($r < r_p$), the soil properties (permeability and soil anisotropy) are altered severely at radial distance where $\Delta u = \sigma'_{v0}$.

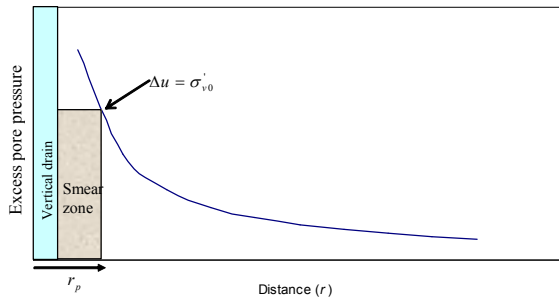


Figure 14 Smear zone prediction by the Cavity Expansion Theory

Based on laboratory tests conducted on a large-scale consolidometer at University of Wollongong, the smear zone extent can be quantified either by permeability variation or water content variation along the radial distance (Indraratna and Redana, 1997; Sathanathan and Indraratna, 2006). Fig. 15 shows the variation of the ratio of the horizontal to vertical permeabilities (k_h/k_v) at different consolidation pressures along the radial distance, obtained from large-scale laboratory consolidation. The variation of the water content with radial distance is shown in Fig. 16. As expected, the water content decreases towards the drain, and also the water content is greater towards the bottom of cell at all radial locations.

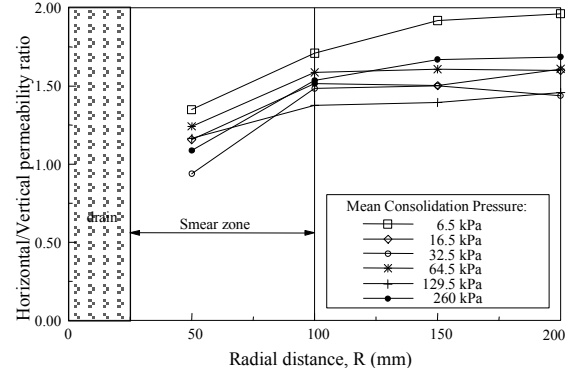


Figure 15 Ratio of k_h/k_v along the radial distance from the central drain (after Indraratna and Redana 1995)

5. THE EFFECT OF DRAIN UNSATURATION DURING INSTALLATION

Unsaturation of soil adjacent to the drain can occur due to mandrel withdrawal (air gap) or application of vacuum pressure through PVDs. Indraratna et al. (2004) attempted to describe the apparent retardation of pore pressure dissipation in large-scale laboratory testing through a series of models, considering the effects of unsaturation at the drain-soil interface.

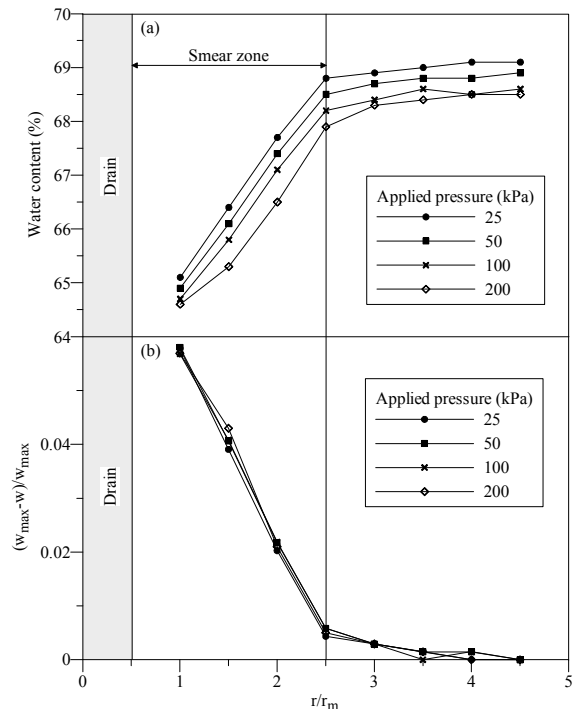


Figure 16 (a) water content, and (b) normalized water content reduction with radial distance at a depth of 0.5 m (after Sathanathan and Indraratna, 2006)

The consolidation behaviour of soft clay in the large-scale consolidometer under combined vacuum and surcharge preloading was analysed using the FEM programme ABAQUS, incorporating the modified Cam-clay theory

(Roscoe and Burland 1968). Fig. 17 illustrates the plane strain finite element discretisation employing 8-noded linear strain quadrilateral elements (CPE8RP) with 8 displacement nodes plus 4 pore pressure nodes. It is sufficient to analyse one half of the cell due to symmetry. The soil moisture characteristic curve (SMCC) including the effect of drain unsaturation was captured by a thin layer of drain elements governed by elastic properties. The converted permeability coefficients based on Indraratna and Redana (2000) method and the apparent past maximum pressure are listed in Table 1.

Table 1. Modified Cam-clay parameters used in consolidometer analysis (Indraratna et al., 2004)

Soil Model Parameters	Values
λ	0.15
κ	0.05
Critical state void ratio, e_{cs}	1.55
Critical state line slope, M	1.1
Permeability in undisturbed zone, k_{hp} (m/s)	9.1×10^{-11}
Poisson's ratio, ν	0.25
Permeability in smear zone, k'_{hp} (m/s)	3.6×10^{-11}

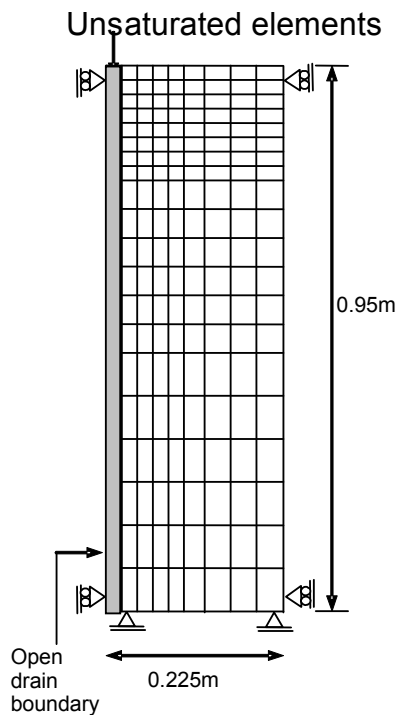


Figure 17 FEM discretisation for plane strain analysis in large-scale consolidometer (Indraratna et al. 2004)

The following 3 models were analysed:

Model 1 – fully saturated soil with linear vacuum pressure distribution along the drain length. The soil behaviour is based on the modified Cam–clay parameters (Table 1).

Model 2 – The soil is initially fully saturated. With the application of linearly varying vacuum pressure, a layer of unsaturated elements is simulated at the PVD boundary. The thin unsaturated layer is modeled elastically ($E = 1000$ kPa, $\nu = 0.25$).

Model 3 – Conditions are similar to Model 2, but the variation of vacuum pressure with time (vacuum removal and reloading) is included.

Fig. 18 shows the surface settlement predicted from the above described models. The predictions prove that the assumption of unsaturated soil layer at the drain-soil boundary with time dependent vacuum pressure variation (Model 3) is justified. Full saturation represented by Model 1 over-predicts the settlement, illustrating the effect of mandrel induced unsaturation.

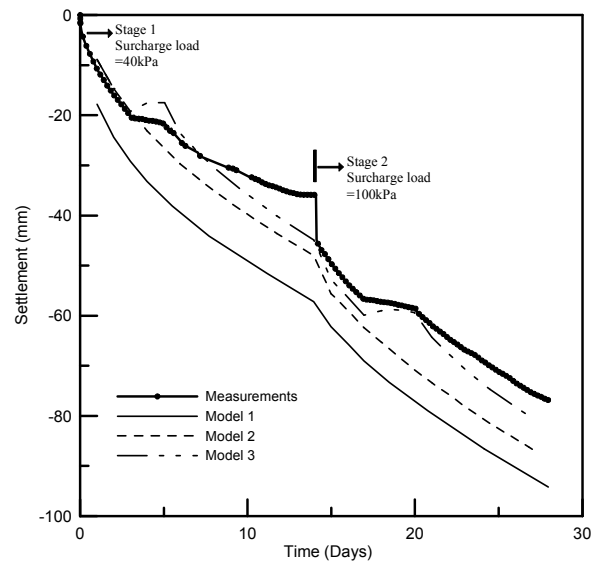


Figure 18 Predicted and measured settlement at the top of consolidometer (Indraratna et al. 2004)

The predicted and measured values of excess pore water pressure (mid layer) are presented in Fig. 19, and Models 2 and 3 agree well with the laboratory observations. As expected, Model 1 (fully saturated) gives the lowest pore pressures, suggesting the unsaturated soil-drain boundary causing the retardation of excess pore water pressure dissipation. In view of both settlements (Fig. 17) and excess pore pressures (Fig. 18), Model 3 provides the most accurate predictions in comparison with the laboratory measurements. There is no doubt, the probable drain unsaturation is an important aspect that should be captured in numerical modelling, especially under vacuum pressure application. The adoption of correct SMCC in finite element analysis is desirable.

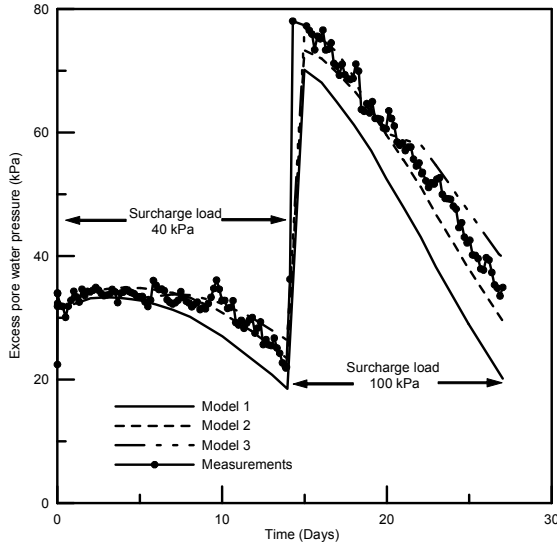


Figure 19 Predicted and measured excess pore water pressure (Indraratna et al. 2004)

6. APPLICATION TO CASE HISTORIES

6.1 Second Bangkok International Airport

6.1.1 Site Characteristics and Embankment Details

The Second Bangkok International Airport (SBIA) has been constructed since 1965 to replace the existing airport. The location of the airport is on a low-lying soft clay. Ground improvement techniques are imperative prior to the airport construction to prevent excessive settlement and lateral movement. Several trial embankments were built at this site, one of them (TV2) was built with PVDs and vacuum application (Asian Institute of Technology, 1995). Fig. 20 illustrates the vertical cross sections and the positions of field instruments, where 12m long PVDs with perforated and corrugated pipes wrapped together in non-woven geotextile were used. The 0.8m sand platform served as a drainage blanket was constructed with an air and water tight linear low density polyethylene (geomembrane) liner placed on top of the drainage system. This liner was sealed by placing its edges at the bottom of the trench perimeter and covered with a 300mm layer of bentonite and then submerged with water.

The extent of the smear zone with depth was predicted using the cavity expansion theory as explained in Section 4. The predicted smear zone variation with depth for each soil layers is shown in Fig. 21.

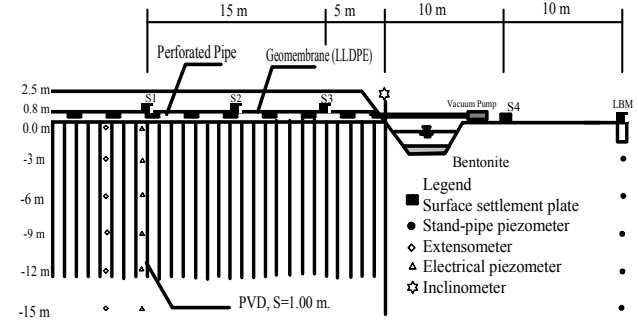


Figure 20 Cross section of embankment TV2 and location of monitoring system (Indraratna et al., 2005d)

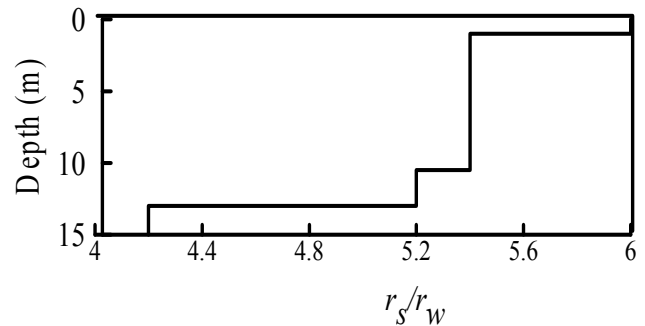


Figure 21 Variation of smear zone with depth by the Cavity Expansion theory (where, r_s : radius of smear zone, and r_w : radius of drain) (Indraratna et al., 2005d)

A vacuum pressure up to 70kPa (equivalent to 4m height of embankment) was applied using the available vacuum equipment. The surcharge load was applied in 4 stages upto 2.5m high (the unit weight of surcharge fill is 18 kN/m^3) as illustrated in Fig. 22. During the application of vacuum pressure, the measured suction head could not be constantly maintained as shown in Fig. 23. This variation has been attributed to air leaks through the surface membrane or the loss of suction head beneath the certain depth for long PVD. Intersection of natural macro-pores with drains at various depths also lead to suction head drops, at various times. The settlement, excess pore water pressure, and lateral movement were recorded 160 days.

6.1.2 Multi-drain Analysis Using FEM Incorporating Proposed Equivalent Plain Strain Model

The consolidation behaviour was analysed using the finite element software ABAQUS. The *equivalent* plane strain model (Equations 14-15) as well as the modified Cam-clay theory (Roscoe and Burland, 1968) were used in the analysis (Indraratna et al., 2005d). The ratios of k_r/k_s and d_s/d_w determined in the laboratory are approximately 1.5-2.0 and 3-4, respectively, however in practice these ratios can vary from 1.5 to 6 depending on the type of drain, mandrel size and shape and installation procedures used (Indraratna and Redana, 2000). The constant values of k_r/k_s and d_s/d_w for this case study were assumed to be 2

and 6, respectively (Indraratna et al., 2004). For the plane strain FEM simulation, the equivalent permeability inside and outside the smear zone was determined using Equations (14) and (15). The discharge capacity (q_w) is assumed high enough and can be neglected (Indraratna and Redana, 2000).

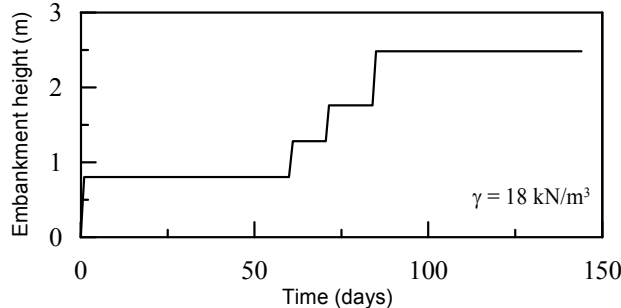


Figure 22 Multi-stage loading (Indraratna et al., 2005d)

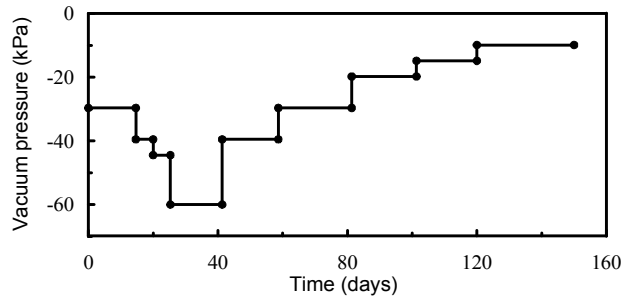


Figure 23 Time dependent vacuum pressure (Indraratna et al., 2005d)

The finite element mesh contained 8-node bi-quadratic displacement and bilinear pore pressure elements (Fig. 24). Only the right hand side of the embankment was modeled due to symmetry, as shown in Fig. 24. The incremental surcharge loading was simulated at the upper boundary.

The following 4 distinct models were numerically examined under the 2D multi-drain analysis (Indraratna et al., 2005d):

Model A: Conventional analysis (i.e., no vacuum application);

Model B: Vacuum pressure varies according to field measurement and decreases linearly to zero at the bottom of the drain ($k_1=0$);

Model C: No vacuum loss (i.e. -60kPa vacuum pressure was kept constant after 40 days); vacuum pressure diminishes to zero along the drain length ($k_1=0$); and

Model D: Constant time-dependent vacuum pressure throughout the soil layer ($k_1=1$).

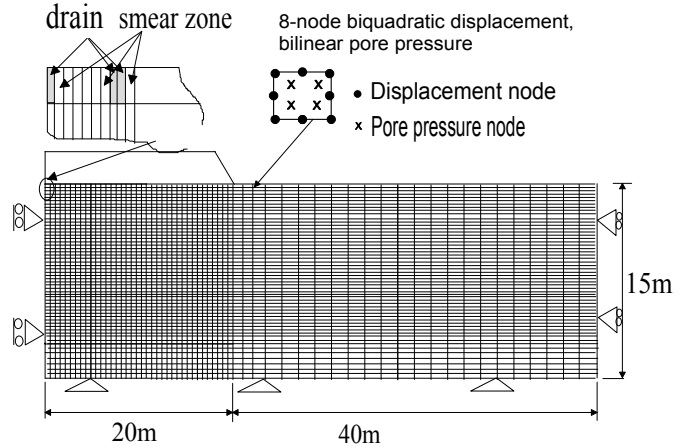


Figure 24 Finite element mesh for plane strain analysis (modified after Indraratna et al. 2005d)

Fig. 25 compares surface settlement between prediction and measurement (centreline). Model B predictions agree with the field data. Comparing all the different vacuum pressure conditions, a vacuum application combined with a PVD system is found to accelerate the consolidation process significantly. With vacuum application, most of the primary consolidation is achieved around 120 days, whereas conventional surcharge (same equivalent pressure) requires more time to complete primary consolidation (after 150 days). It is also apparent that a greater settlement can be obtained, if any loss of vacuum pressure can be minimised (Model C).

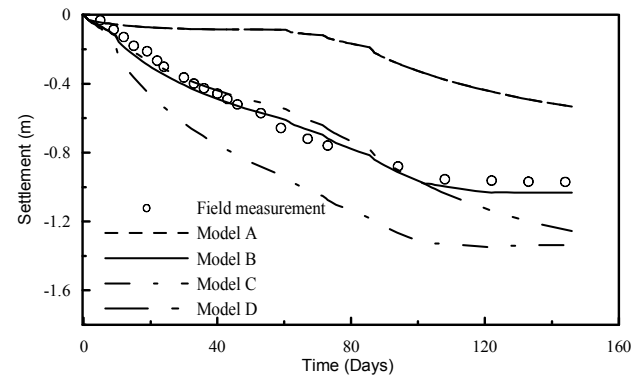


Figure 25 Surface settlements (modified after Indraratna et al., 2005d)

Fig. 26 presents the predicted and measured excess pore pressures. The field observations are closest to Model B, implying that the authors' assumption of linearly decreasing time-dependent vacuum pressure along the drain length is justified. Excess pore pressure generated from the vacuum application is less than the conventional case, which enables the rate of construction of an embankment to be higher than conventional construction.

The predicted and measured lateral displacements (at the end of embankment construction) are shown in Fig. 27.

As described by Indraratan et al. (2005d), the observed lateral displacements do not agree well with all vacuum pressure models. In the middle of the very soft clay layer (4-5m deep), the predictions from Models B and C are closest to the field measurements. Nearer to the surface, the field observations do not agree with the 'inward' lateral movements predicted by Models B and C. The discrepancy between the finite element models and the measured results is more evident in the topmost weathered crust (0-2 m).

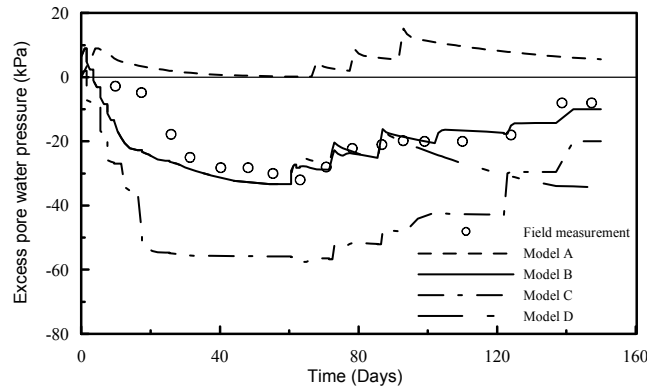


Figure 26 Variation of excess pore water pressure at 3m below the surface and 0.5m away from centreline (modified after Indraratna et al., 2005d)

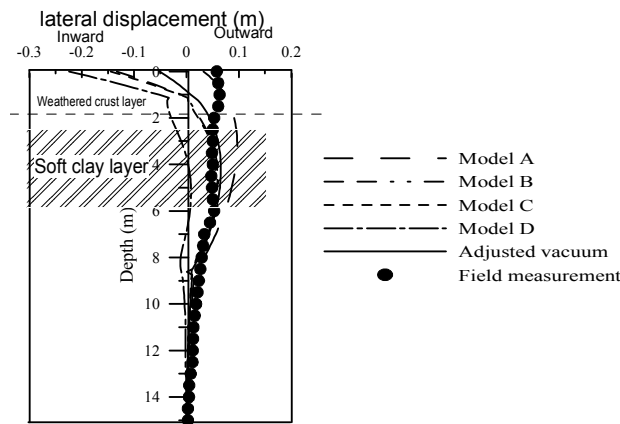


Figure 27 Calculated and measured lateral displacements distribution with depth (modified after Indraratna et al., 2005d)

As discussed by Indraratna et al., 1997, if vertical drains are not provided and the surcharge embankment is raised quickly, it can fail in 13 days in the absence of effective pore pressure dissipation. In contrast, the same clay formation stabilised with PVDs shows insignificant lateral displacement after 13 days. Even after 7 years, the normalised lateral displacements will be less than that without PVDs (Fig. 28). Normalised lateral displacement is the absolute lateral displacement divided by the maximum embankment height.

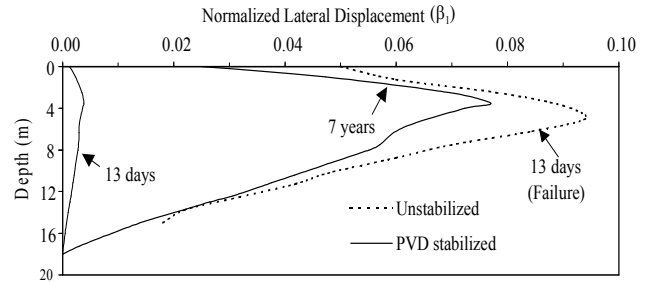


Figure 28 Curtailing lateral displacements due to PVDs (after Indraratna et al., 1997)

6.2 Ska-Edeby Embankment, Stockholm, Sweden

The practical application of non-Darcian plane strain solution is demonstrated through a well documented pilot study (Ska-Edeby, 25 km west of Stockholm, Sweden). The site details including the construction history and soil parameters are given elsewhere by Hansbo, 1997; 2005. Here, for the purpose of discussion, Area II with an equivalent loading of 32 kPa is selected. Sand drains of 180 mm diameter are installed in an equilateral triangular pattern at 1.5 m spacing (i.e. $D=1.58$ m).

In Figure 29, the estimated degree of consolidation based on the Darcian axisymmetric, non-Darcian axisymmetric (Hansbo, 1997) and non-Darcian plane strain solutions (Sathanathan and Indraratna, 2005) are plotted with the available field data at embankment centerline. The predicted values based on non-Darcian flow seem to agree better with the field data in relation to the Darcian (conventional) analysis. However, in the opinion of the authors, this difference is usually small, and for all practical purposes the conventional Darcy conditions are sufficient.

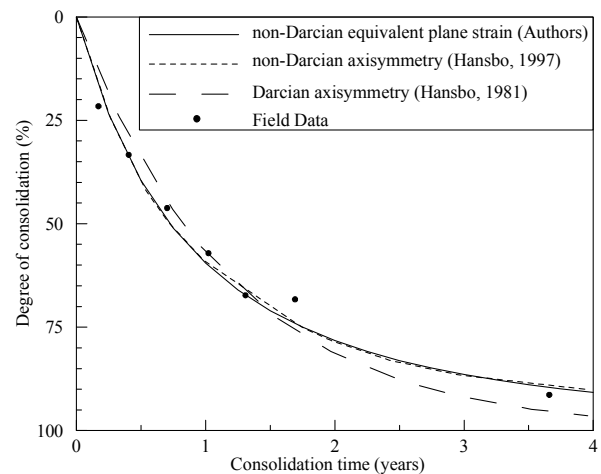


Figure 29 Degree of consolidation at the embankment centreline with time for Area II, Ska-Edeby field study (after Hansbo, 2005; Sathanathan & Indraratna, 2005)

7. PERFORMANCE OF SHORT VERTICAL DRAINS SUBJECTED TO CYCLIC TRAIN LOADS

Low-lying areas with high volumes of plastic clays can sustain high excess pore water pressures during both static and cyclic (repeated) loading. The effectiveness of prefabricated vertical drains (PVD) for dissipating cyclic pore water pressures is discussed here. In poorly drained situations, the increase in pore pressures will decrease the effective load bearing capacity of the formation. Even if the rail tracks are well built structurally, undrained formation failures can adversely influence the train speeds apart from the inevitable operational delays. Under circumstances of high excess pore water pressures, clay slurring may be initiated pumping the slurred soil upwards under cyclic loads, clogging the clean ballast and causing poor drainage.

As described earlier, PVDs accelerate consolidation and curtail lateral movements. The stability of rail tracks and highways built on soft saturated clays is often governed by the magnitude of lateral strains, even though consolidation facilitates a gain in shear strength and load bearing capacity. If excessive initial settlement of deep estuarine deposits cannot be tolerated in terms of maintenance practices (e.g. in new railway tracks where continuous ballast packing may be required), the rate of settlement can still be controlled by: (a) keeping the drain length relatively short, and (b) optimising the drain spacing and the drain installation pattern. In this way, while the settlements are acceptable, the reduction in lateral strains and gain in shear strength of the soil beneath the track improve its stability significantly.

7.1 Laboratory testing

A large-scale triaxial test was used to examine the effect of cyclic load on the radial drainage and consolidation by PVDs (Fig. 30a). This testing chamber is capable of accommodating specimens of 300 mm diameter and 600 mm high (Fig. 30b). The excess pore water pressure was monitored via miniature pore pressure transducers. These instruments were saturated under deaired water with vacuum pressure, and then fitted through the base of the cell to the desired sample locations.

A reconstituted estuarine clay was tested. The sample was lightly compacted to a unit weight of about 17 to 17.5 kN/m³. Ideally, testing requires the simulation of k_0 conditions that may typically vary in the range of 0.6-0.7 in many coastal regions of Australia. Most soft clays will have natural water contents exceeding 75%, and Plasticity Index above 35%. It is not uncommon to find undrained shear strengths of softest estuarine deposits to be less than 8 kPa. In Northern Queensland, some very soft clays that have caused embankment problems have been characterised by c_u values less than 5 kPa.



Figure 30 (a) Large-scale triaxial rig, (b) soil specimen

The tests could be conducted at frequencies of 5-10 Hz, typically simulating train speeds of say 60-100 km/h of 25-30 tonnes/axle train loads. Fig. 31 shows an example of the excess pore pressure recorded, which indicates that the maximum excess pore water pressure beside the PVD during the cyclic load application (T4) are significantly less compared to that near the cell boundary (T3). Also as expected, the excess pore pressures close to the outer cell boundary (e.g. T1 and T3) dissipated at a slower rate than T4 and T2 closer to the PVD. The test results reveal that PVDs decrease the maximum excess pore pressure effectively even under cyclic loading.

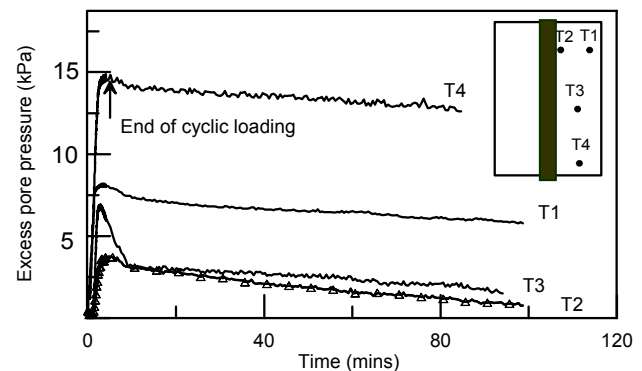


Figure 31 Dissipation of excess pore pressure at various locations from the PVD

7.2 Numerical analysis

Attempts to consolidate deep estuarine soft clays (up to 30-40m) may take a very long time and often uneconomical, especially when relatively high surcharge embankments cannot be raised rapidly due to obvious stability problems. Under railway tracks, where the significant proportion of the applied load is usually sustained within the first several meters of the formation, assuming sufficient ballast and subballast depths are provided. In this regard, there is no need for improving

the entire depth of soft clay deposit, hence, relatively short PVDs without prolonged preloading may still be adequate in design. Short PVDs (5-8m) may still dissipate the cyclic pore pressures, curtail the lateral movements and increase the shear strength and bearing capacity of the soft formation to a reasonable depth below the sub-ballast. In other words, this will provide a “stiffened” section of the soft clay up to several meters in depth, supporting the rail track within the predominant influence zone of vertical stress distribution.

In railway engineering, repeated train loading is usually modelled as a static load corrected by an impact load factor (dynamic amplification factor). The value of impact load factor may be changed according to the field conditions simulated on track (Esveld, 2001). In the following example, a static load of 80kPa with an impact factor of 1.3 is applied. A typical cross-section of the formation beneath the rail track is shown in Fig. 32, where a relatively shallow very soft clay deposit is underlain by a deeper soft soil layer of slightly higher stiffness. PVDs are only used to stabilize the shallow soil layer immediately beneath the track. A FEM, 2D plane strain model (Indraratna and Redana, 2000) using triangular elements with 6 displacement nodes and 3 pore pressure nodes is considered.

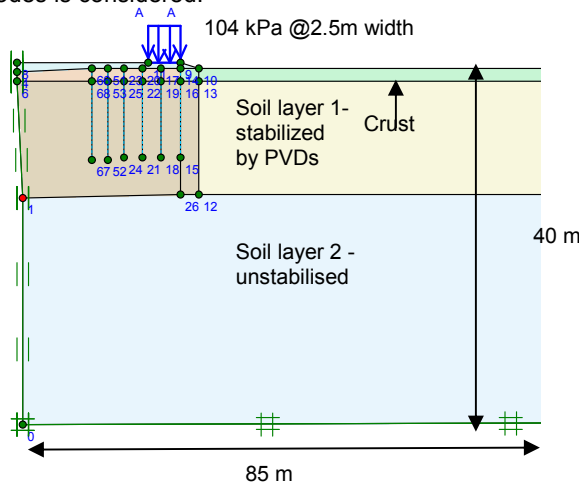


Figure 32 Vertical cross section of track and formation

Soil Properties are summarised in Table 2. Top compacted soil crust including sub-ballast fill (1m in thickness) and the ballast layer (300mm thick) are modelled by Mohr-Coulomb theory. The two layers of soft normally consolidated clays are conveniently modelled using the modified Cam-clay theory (Roscoe and Burland, 1968). For typical track conditions, unit weight of artificially compacted granular fills is assumed around 16.5-17 kN/m³ with a deformation modulus not more than 200 MPa. The saturated unit weights of the soft clay layers is assumed to be 15.5-16 kN/m³ (deeper soil layer having the higher unit weight).

Table 2. Assumed parameters for soft soil foundation and ballasted track (300mm of ballast thickness and 1m thick compacted fill and crusted layer)

Depth of layer (m)	Model	c (kPa)	ϕ (degree)	$\lambda/(1+e_0)$	$\kappa/(1+e_0)$
+0.3	M-C	5	45		
0-1	M-C	29	29		
1-10	S-S	10	25	0.15	0.03
10-30	S-S	15	20	0.12	0.02

Note: M-C= Mohr-Coulomb, S-S= Soft Soil

The rapid dissipation of excess pore water pressure due to PVDs is clearly beneficial. More than 65% excess pore pressure dissipation is seen within first 4-5 months (Fig. 33). In the absence of preloading embankment or vacuum preloading, the corresponding initial settlements induced by short PVDs is less than 0.5m after about 3 months. This settlement can still be acceptable over a routine maintenance period by packing more ballast with time. More significant is the considerable reduction of lateral displacement in the PVD stabilised soil underlying the compacted crust (Fig. 34). While long-term lateral displacements at shallow depths (@ 3m) could be as large as 250-300mm, the PVDs are shown to decrease the lateral displacement by about 25%. This numerical example demonstrates the role of short PVDs installed beneath rail tracks.

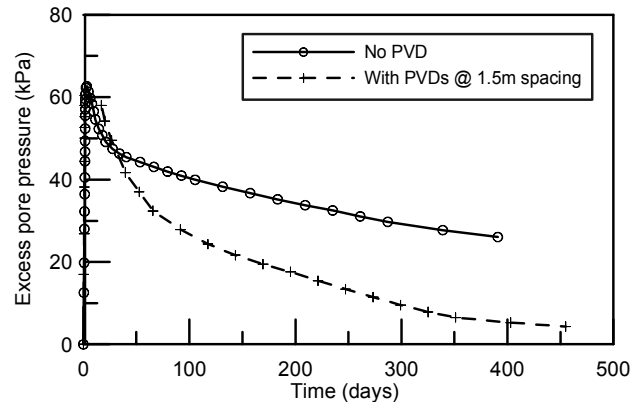


Figure 33 Excess pore pressure dissipation at 2 m depth at centre line of rail track

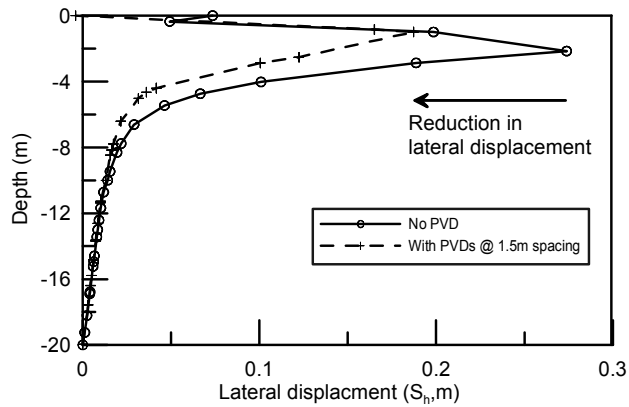


Figure 34 Ultimate lateral displacement profiles near the embankment toe

7.3 Soil Improvement for Tsunami Devastated areas

The Boxing Day tsunami in December 2004 devastated several South and Southeast Asian countries, including Sri Lanka, Indonesia and Thailand. The effect of tsunami waves on the surface soils is briefly discussed here, in view of the ground improvement needs for reconstruction of infrastructure including roads and railways. The first author was an invited expert in the post-tsunami site investigations of the devastated southern coast of Sri Lanka, and various soil testing was conducted under his guidance. At a trial pit beside a major rail disaster (more than 1000 casualties in the overturned and damaged train carriages), the particle size distributions (Fig. 35) indicated blended and significantly more well-graded nature of the fine sandy soils close to the surface, in the areas where uniform and relatively clean fine beach sand existed before the tsunami. The uniformity coefficient has changed from 1.6 to 4.6 in this particular location as a result of considerable turbulent mixing.

Also near the same locations, standard cone penetrometer testing with pore pressure measurement (CPTU) was conducted to re-examine the soil profile up to about 10m deep (e.g. Fig. 36). The friction ratios determined for shallow depths (less than 1m) confirm remoulded, metastable sands and/or mixed fine grained soils (marine silts and clays transported by waves) with increased sensitivity. The presence of peat is identified by the suddenly increased friction ratio. The test results also indicated significantly increased water content of the soil affected by the infiltration of water (Fig. 36). The extreme remoulding by tsunami waters and the blending of fine marine muds (transported) with fine beach has resulted in a significant decrease in the original unit weight as well as causing relatively poor drainage conditions (i.e. compared to the pre-tsunami era, the surface soil is not free-draining anymore). Increased degree of saturation now allows excess pore pressures to be developed and sustained upon loading. In such situations, the ground improvement benefits from conventional vibratory compaction and preloading to increase the shear strength. Particularly in railway track areas, the use of short PVDs will be most advantageous for dissipating

cyclic pore pressures and curtailing lateral displacements as described earlier.

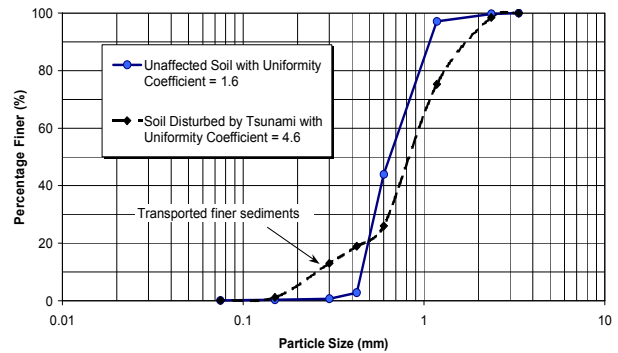


Figure 35 Particle size distribution curves of the tsunami affected and unaffected soils

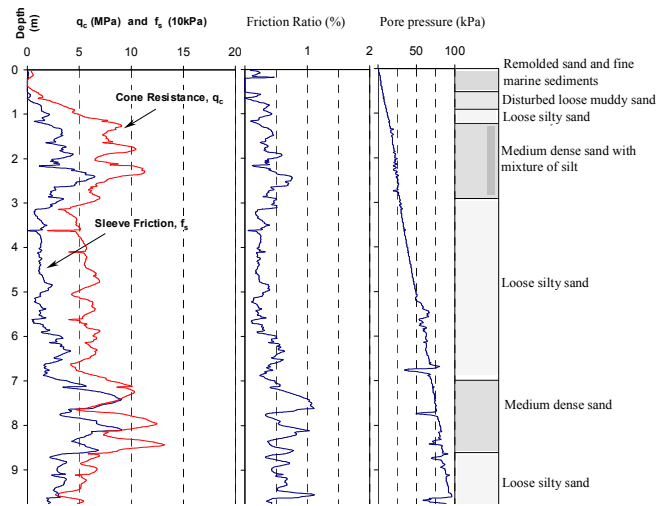


Figure 36 Cone penetration test with pore pressure (CPTU) results of soil layers after tsunami occurrence

The use of short PVDs to facilitate the dissipation of cyclic pore pressures are imperative to consider through sound research evidence.

8. USE OF NATIVE VEGETATION ON THE STABILISATION OF SOFT FORMATIONS

The tree roots provide an effective form of natural soil reinforcement apart from dissipating the excess pore water pressure, and generate sufficient matric suction to increase the shear strength of the surrounding soil. In Australia, various forms of native vegetation grow along rail corridors. It is well recognised that such biostabilisation has a number of mechanical and hydrological effects on ground stability. The loss of moisture from the soil due to uptake by tree roots may be categorized as: (a) water used for metabolism in plant tissues, and (b) water transpired to the atmosphere from the canopy (foliage). In order to quantify pore pressure

dissipation and induced matric suction, Indraratna et al. (2006) introduced an appropriate mathematical model for considering soil suction, root density and potential transpiration (Fig. 37).

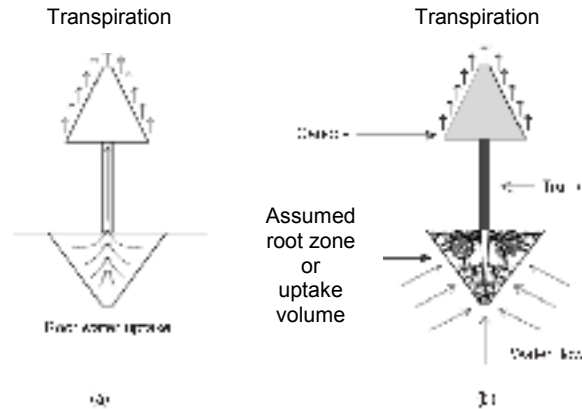


Figure 37 Schematic sketch of soil–plant–atmosphere equilibrium: (a) transpiration; (b) soil–plant–atmosphere interaction (Indraratna et al., 2006)

8.1 Conceptual Modelling

The main variable for estimating the transpiration rate is the rate of root water uptake, which is difficult to assess because of the considerable variation of root geometry from one species to another. In this section, the key factors, such as soil suction, root distribution and potential transpiration rate are briefly discussed.

8.1.1 Soil suction

Soil suction retards the free water movement towards the root zone and affects the transpiration rate. The root water uptake ($S(x, y, z, t)$) is represented by a combined function of the maximum possible root water uptake, S_{\max} , and matric suction, ψ :

$$S(x, y, z, t) = S_{\max}(x, y, z, t)f(\psi) \quad (34)$$

$S(x, y, z, t)$ denotes the root water uptake at point (x, y, z) at time t .

8.1.2 Root distribution

In the development of the model, the geometric slope of the root zone has to be assumed, based on the field observation of typical root cross sections. Trench excavation is one of the appropriate methods to map the root density distribution (Fig. 38). The distribution of transpiration within the root zone depends on the root density, hence,

$$S(x, y, z, t) = f(\psi)G(\beta)F(T_p) \quad (35)$$

where, $G(\beta)$ is a function associated with the root density distribution, $F(T_p)$ is a function to consider the potential transpiration distribution, and $\beta(x, y, z, t)$ is the root density.



Figure 38 Trench excavation to examine the root density distribution of a native tree (Miram, VIC, Australia)

8.1.3 Potential transpiration

The potential transpiration is defined as evaporation of water from plant tissues to the atmosphere, assuming that the soil moisture content is not restricted. The potential transpiration is, therefore, estimated by:

$$T_p = ET_p - E_p \quad (36)$$

where, T_p is overall transpiration, ET_p is the potential evapotranspiration (both plant and soil), and E_p is the potential evaporation from the soil surface.

The finite element program ABAQUS was used to evaluate the soil suction generated by transpiration. Equations (34)-(36) are incorporated as a sub-routine in ABAQUS supplementing the effective stress-based equations.

8.2 Verification of the Proposed Root Water Uptake Model

To verify the model for rate of root water uptake, a case history reported by Biddle (1983) has been considered for a lime tree grown in Boulder clay. The estimated parameters based on the available literature are shown in Table 3. Fig. 39 illustrates the mesh and element geometry and boundary conditions of the finite element model. A two-dimensional plane strain mesh employing 4-node bilinear displacement and pore pressure elements (CPE4P) was considered. The maximum change in the soil matric suction from the finite element analysis (fig. 40) is found at about 0.5m depth, which coincides with the same location of the maximum root density.

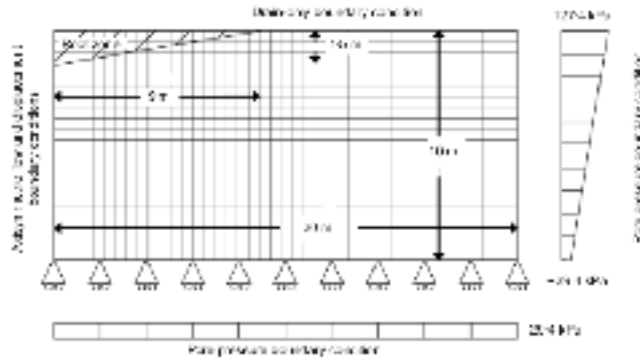


Figure 39 Geometry and boundary conditions (Indraratna et al., 2006)

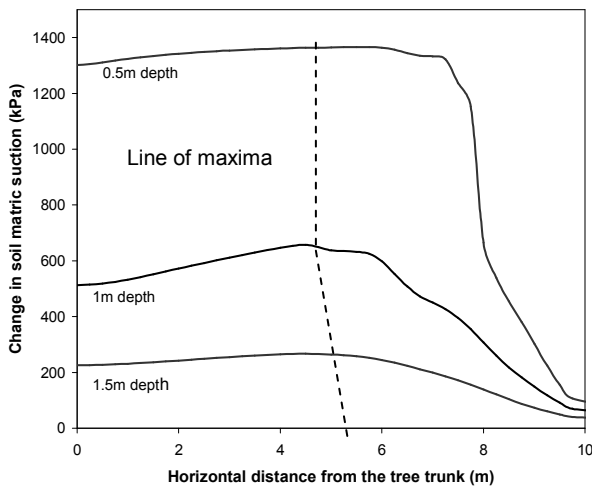


Figure 40 Predicted soil matric suction in various depths (Indraratna et al., 2006)

A comparison between the field measurements and the FEM predictions for moisture content reduction around the lime tree is presented in Fig. 41. The numerical model is in accordance with the field observations by Biddle (1983). The main differences noted between field data and the predictions are observed at 6-8m from the trunk. This discrepancy is attributed to the simplicity of the assumed root zone shape. In addition, the foliage prevents uniform distribution of rainfall around the tree.

As a result, moisture content can increase at the canopy edges, thereby further contributing to this disparity

Table 3. Parameter used in the finite element analysis (Indraratna et al., 2006)

Parameter	Value	Reference
r_{\max}	9m	Biddle (1983)
z_{\max}	1.5m	Biddle (1983)
PI	23	Biddle (1983)
ψ_{an}	4.9 kPa	Feddes et al. (1978)
ψ_w	1500 kPa	Feddes et al. (1978)
ψ_d	40 kPa	Feddes et al. (1978)
e_0	0.60	Powrie et. al (1992)
γ	21 kN/m ³	Powrie et. al (1992)
C_c	0.13	Skempton (1944)
k_s	10 ⁻¹⁰ m/s	Lehane and Simpson (2000)

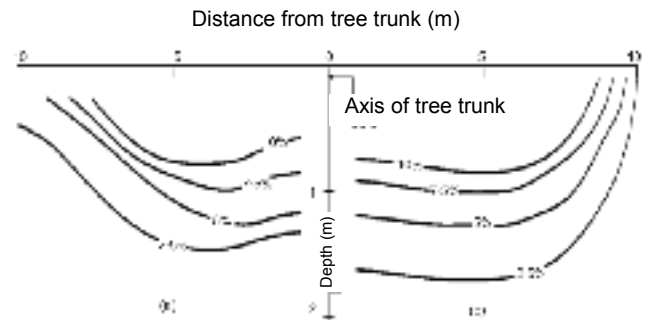


Figure 41 Contours of volumetric soil moisture content reduction (%) close to a lime tree: (a) Biddle (1983), (b) FEM predictions (Indraratna et al., 2006)

Fig. 42 shows the ground settlement at various depths. In this analysis, only the suction related settlement was considered. On the surface, the predicted 80mm settlement beside the tree trunk decreases to less than 20 mm, at a distance 10 m away from the trunk. As shown in Fig. 42, the location of the maximum settlement is closer to the trunk at shallower depths, which tends to coincide with the points of maximum change in suction (Fig. 40).

It was shown that the numerical analysis incorporating the proposed model could predict the variation of moisture content surrounding the tree trunk. Knowing the moisture content variation, the development of matric suction can be predicted reasonably well using the SMCC. Native biostabilisation improves the shear strength of the soil by increasing the matric suction, and also decreases the soil movements. This contribution from trees grown along rail corridors and rail slope is of immense benefit for improving track stability in problematic soil. In other words, native vegetation generating soil suction is comparable to the role of PVDs with vacuum pressure, in

terms of improved drainage (pore water dissipation), and associated increase in shear strength. In addition, the tree roots provide a natural reinforcement effect, which the current model has not simulated thus far.

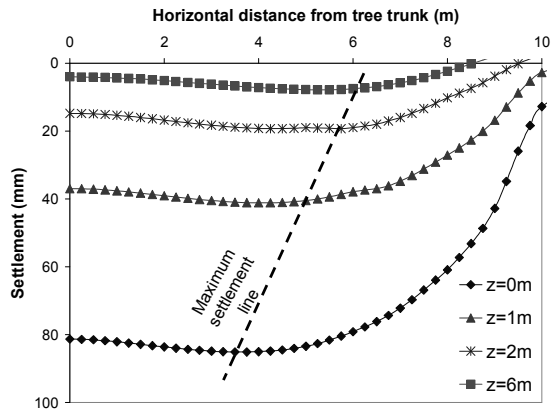


Figure 42 Ground settlement at various depths

9. CONCLUSIONS

For several decades, various types of vertical drains have been used to accelerate the rate of primary consolidation. A revised mathematical model for soft clay stabilised by vertical drains incorporating the compressibility indices (C_c and C_r) and vacuum surcharge has been introduced. The variation of horizontal permeability coefficient (k_h) was represented by the e - $\log k_h$ relationship. The variables such as the slopes of the e - $\log \sigma'$ relationship (C_c and C_r), the slope of e - $\log k_h$ relationship (C_k), vacuum pressure ratio (VPR) and the loading increment ratio ($\Delta p/\sigma'_i$) were explicitly integrated in the mathematical model to predict the consolidation behaviour.

The lateral displacements and pore pressures dissipation associated with PVDs are often difficult to predict accurately. This may be attributed to the complexity of evaluating the true magnitudes of soil parameters inside and outside the smear zone, correct drain properties as well as the aspects of soil-drain interface unsaturation. Therefore, one needs to use the most appropriate laboratory techniques to obtain parameters, preferably using large-scale testing equipment. It was found that the smear zone radius was 2-3 times the radius of the mandrel. The soil permeability in the smear zone is higher than that in the undisturbed zone by a factor of 1.5-2.

For large construction sites, where many PVDs are installed, the plane strain analysis is sufficient given the computational efficiency. Recently developed conversion from axisymmetric to plane strain condition gives good agreement with measured data. These simplified plane strain methods can be rapidly employed in the numerical analysis. A finite element code (ABAQUS) was employed to analyse the behaviour of PVDs and compared with field measurements. A conversion procedure based on the transformation of permeability and vacuum pressure was also proposed to establish the relationship between

the axisymmetric (3D) and equivalent plane strain (2D) conditions. The equivalent plane strain solution was applied for selected case histories, demonstrating its validity in predicting the real behaviour. Field behaviour as well as model predictions indicate that the efficiency of vertical drains depends on the magnitude and distribution of vacuum pressure as well as the degree of drain saturation during installation.

The accurate prediction of lateral displacement at shallow depths depends on the correct assessment of soil properties including the overconsolidated surface crust. This compacted layer is relatively stiff, and therefore it resists 'inward' movement of the soil upon the application of vacuum pressure. The modified Cam-clay model is inappropriate for modeling the behavior of the weathered and compacted crust. This surface crust is sufficient to be modeled as an elastic layer rather than a 'soft' elastoplastic medium. The analysis of case histories proves that the vacuum application via PVD substantially decreases lateral displacement. As a result, the potential shear failure during rapid embankment construction can be avoided.

There is no doubt that a system of vacuum-assisted consolidation via PVDs is a useful and practical approach for accelerating radial consolidation. Such a system eliminates the need for a high surcharge load, as long as air leaks can be prevented in the field. Accurate modeling of vacuum preloading requires both laboratory and field studies to quantify the nature of vacuum pressure distribution within a given formation and drain system.

The ground improvement techniques including PVDs prior to rail track construction can be applied in coastal areas containing a high percentage of clayey soils. It was shown that short prefabricated vertical drains (PVDs) can be used under rail tracks to dissipate cyclic excess pore pressure and curtail lateral displacements to improve stability. Native vegetation can also be used close to the rail track to reduce settlement and lateral movement. The proposed root water uptake and transpiration model verifies that the suction induced by the tree roots contributes to a substantial gain shear strength. Similar to PVDs, the tree roots induce good drainage, pore water pressure dissipation and in addition provide natural reinforcement of the soil. As the influence zone of each tree can be several meters in radius, the methodological planting of native trees along rail corridors at a practical distance away from the track is currently considered by rail organizations in Australia. Considering various soil conditions, the type of vegetation and atmospheric conditions, the proposed mathematical model for biostabilisation is most useful to predict the formation behaviour in a rail track environment.

10. ACKNOWLEDGEMENTS

The authors wish to thank the CRC for Railway Engineering and Technologies (Australia) for its continuous support. Cyclic testing of PVD stabilised soft soil forms a part of Anaas Attya's doctoral thesis. Extensive research on biostabilisation by native trees is

currently conducted by doctoral student Behzad Fatahi. A number of other current and past doctoral students, namely, Redana, Bamunawita, and Sathananthan have also contributed to the contents of this keynote paper. More elaborate details of the contents discussed in this paper can be found in previous publications of the first author and his research students in ICE proceedings (Geotechnical Engineering), ASCE and Canadian Geotechnical Journals, since mid 1990's.

11. REFERENCES

- AIT. 1995. The Full Scale Field Test of Prefabricated Vertical Drains for The Second Bangkok International Airport (SBIA). AIT, Bangkok, Thailand.
- Barron, R.A. 1948. Consolidation of fine-grained soils by drain wells. Transactions ASCE, Vol. 113, pp. 718-754.
- Biddle P.G. 1983. Pattern of soil drying and moisture deficit in the vicinity of trees on clay soils. Geotechnique, Vol. 33, No. 2, pp.107-126.
- Bo, M. W., Chu, J., Low, B. K., and Choa, V. 2003. Soil improvement; prefabricated vertical drain techniques, Thomson Learning, Singapore.
- Broms, B. 1987. Soil improvement methods in Southeast Asia for soft soils. Asian regional conference on soil mechanics and foundation engineering, Kyoto, Japan, Vol. 2, pp. 29-64.
- Cao, L. F., Teh, C. I., and Chang, M. F. 2001. Undrained Cavity Expansion in Modified Cam Clay I: Theoretical Analysis." Geotechnique, Vol. 51, No. 4, pp. 323-334.
- Chu, J., and Yan, S.W. 2005. Application of vacuum preloading method in soil improvement project. Case Histories Book (Volume 3), Edited by Indraratna, B. and Chu, J., Elsevier, London, pp. 91-118.
- Chu, J., Yan, S.W. and Yang, H. 2000. Soil improvement by the vacuum preloading method for an oil storage station. Geotechnique, Vol. 50, No. 6, pp. 625-632.
- Collins, I. F. and Yu, H. S. 1996. Undrained Cavity Expansion in Critical State Soils. International Journal for Numerical and Analytical Methods in Geomechanics, Vol. 20, pp. 489-516.
- Feddes, R.A., Kowalik, P. J. and Zaradny, H. 1978. Simulation of field water use and crop yield. Simulation Monograph. Pudoc, Wageningen, pp. 9-30
- Gabr M.A., and Szabo D.J. 1997. Prefabricated vertical drains zone of influence under vacuum in clayey soil. Proceedings of the Conference on In Situ Remediation of the Geoenvironment, ASCE, 449-460.
- Hansbo, S. 1979. Consolidation of clay by band-shaped prefabricated drains. Ground Eng., Vol. 12, No. 5, pp. 16-25.
- Hansbo, S. 1981. Consolidation of fine-grained soils by prefabricated drains. In Proceedings of 10th International Conference on Soil Mechanics and Foundation Engineering, Stockholm, Balkema, Rotterdam, 3, pp. 677-682.
- Hansbo, S. 1997. Aspects of vertical drain design — Darcian or non-Darcian flow. Géotechnique Vol. 47, No. 5, pp. 983–992.
- Hansbo, S. 2005. Experience of consolidation process from test areas with and without vertical drains. Ground Improvement–Case Histories Book (Volume 3), Edited by Indraratna, B. and Chu, J., Elsevier, London, Chapter 1. pp. 3-49.
- Holtz, R.D., Jamiolkowski, M., Lancellotta, R. and Pedroni, S. 1991. Prefabricated vertical drains: design and performance, CIRIA ground engineering report: ground improvement. Butterworth-Heinemann Ltd, UK, 131 p.
- Hird C.C., Pyrah I.C., and Russel D. 1992. Finite element modeling of vertical drains beneath embankments on soft ground. Geotechnique, Vol. 42(3), pp. 499-511.
- Holtan, G.W. 1965. Vacuum stabilization of subsoil beneath runway extension at Philadelphia International Airport. In Proc. of 6th ICSMFE, 2.
- Indraratna B., and Chu J. 2005. Ground Improvement – Case Histories Book (Volume 3), Elsevier, London 1115p.
- Indraratna B., and Redana I.W. 1997. Plane strain modeling of smear effects associated with vertical drains, Journal of Geotechnical and Geoenvironmental Engineering, ASCE, Vol. 123(5), pp. 474-478.
- Indraratna, B., and Redana, I. W. 1998. Laboratory determination of smear zone due to vertical drain installation. J. Geotech. Eng., ASCE, Vol. 125 No. 1, pp. 96-99.
- Indraratna, B., and Redana, I. W. 2000. Numerical modeling of vertical drains with smear and well resistance installed in soft clay. Canadian Geotechnical Journal, Vol. 37, pp. 132-145.
- Indraratna, B., Balasubramaniam, A. S. and Balachandran, S. 1992a. Performance of test embankment constructed to failure on soft marine clay. Journal of Geotechnical Engineering, ASCE, Vol. 118, No. 1, pp. 12-33.
- Indraratna, B., Balasubramaniam, A., Phamvan, P. and Wong, Y.K. 1992b. Development of Negative Skin Friction on Driven Piles in Soft Clay. Canadian Geotechnical Journal, Vol. 29, June issue, pp. 393 - 404.
- Indraratna, B., Balasubramaniam, A. S., and Ratnayake, P. 1994. Performance of embankment stabilized with

- vertical drains on soft clay. *J. Geotech. Eng., ASCE*, Vol. 120, No. 2, pp. 257-273.
- Indraratna, B., Balasubramaniam, A. S. and Sivaneswaran, N. 1997. Analysis of settlement and lateral deformation of soft clay foundation beneath two full-scale embankments. *International Journal for Numerical and Analytical Methods in Geomechanics*, Vol. 21, pp. 599-618.
- Indraratna, B., Bamunawita, C., and Khabbaz, H. 2004. Numerical modeling of vacuum preloading and field applications. *Canadian Geotechnical Journal*, Vol. 41, pp. 1098-1110.
- Indraratna, B., Rujikiatkamjorn C., and Sathananthan, I., 2005a. Analytical modeling and field assessment of embankment stabilized with vertical drains and vacuum preloading. The Proceedings of the 16th International Conference on Soil Mechanics and Geotechnical Engineering, 12-16 September 2005, Osaka, Japan, Edited by the 16th ICSMGE committee, Millpress, Rotterdam, the Netherlands. pp. 1049-1052.
- Indraratna, B., Rujikiatkamjorn C., and Sathananthan, I. 2005b. Analytical and numerical solutions for a single vertical drain including the effects of vacuum preloading. *Canadian Geotechnical Journal*, Vol. 42, pp. 994-1014.
- Indraratna, B., Rujikiatkamjorn C., and Sathananthan, I. 2005c. Radial consolidation of clay using compressibility indices and varying horizontal permeability. *Canadian Geotechnical Journal*, Vol. 42, pp. 1330-1341.
- Indraratna, B., Rujikiatkamjorn C., Balasubramaniam, A. S. and Wijeyakulasuriya, V. 2005d. Predictions and observations of soft clay foundations stabilized with geosynthetic drains and vacuum surcharge. *Ground Improvement – Case Histories Book (Volume 3)*, Edited by Indraratna, B. and Chu, J., Elsevier, London, pp. 199-230.
- Indraratna, B., Sathananthan, I., Rujikiatkamjorn C. and Balasubramaniam, A. S. 2005e. Analytical and numerical modelling of soft soil stabilized by PVD incorporating vacuum preloading. *International Journal of Geomechanics*, Vol. 5 No. 2, pp. 114-124.
- Indraratna, B., Sathananthan, I., Bamunawita, C. and A.S. Balasubramaniam. 2005f. Theoretical and Numerical Perspectives and Field Observations for the Design and Performance Evaluation of Embankments Constructed on Soft Marine Clay. *Ground Improvement–Case Histories Book (Volume 3)*, Edited by Indraratna, B. and Chu, J., Elsevier, London, Chapter 2. pp. 61-106.
- Indraratna, B., Fatahi, B. and Khabbaz, H. 2006. Numerical analysis of matric suction effects of tree roots. *Proceedings of the Institution of Civil Engineers Geotechnical Engineering*, Vol 159 No. GE2, pp. 77–90.
- Jamiolkowski, M., Lancellotta, R., and Wolski, W. 1983. Precompression and speeding up consolidation. *Proc. 8th ECSMFE*, pp. 1201-1206.
- Johnson, S. J. 1970. Precompression for improving foundation soils. *J. Soil. Mech. Found. Div., ASCE*, Vol.96, No. 1, pp. 111-114.
- Kjellman, W. 1948. Accelerating consolidation of fine grain soils by means of cardboard wicks. *Proc. 2nd ICSMFE*, 2, pp. 302-305.
- Lehane, B.M. and Simpson, B. 2000. Modelling glacial till under triaxial conditions using a BRICK soil model" *Canadian Geotechnical Journal*, Vol. 37, pp. 1078-1088.
- Long, R.P. and Covo, A. 1994 Equivalent diameter of vertical drains with an oblong cross section. *J. Geotech. Eng. Div., ASCE*, Vol. 120, No. 9, pp. 1625-1630.
- Mohamedelhassan E., and Shang, J.Q. 2002. Vacuum and surcharge combined one-dimensional consolidation of clay soils, *Canadian Geotechnical Journal*, **39**: 1126-1138.
- Pradhan, T.B.S., Imai, G., Murata, T., Kamon, M. and Suwa, S. 1993 Experiment study on the equivalent diameter of a prefabricated band-shaped drain. *Proc. 11th Southeast Asian Geotech. Conf.*, Vol. 1, pp. 391-396.
- Nagaraj, T.S., Pandian, N.S. and Narashima Raju, P.S.R. 1994. Stress-state-permeability relations for overconsolidated clays. *Géotechnique*, Vol. 44(2), pp. 349-352.
- Powrie, W., Davies, J.N., and Britto, A. M. 1992. A cantilever retaining wall supported by a berm during temporary work activities. *ICE conference on retaining structures*, Robinson College, Cambridge, pp. 418-428.
- Qian, J.H., Zhao, W.B., Cheung, Y.K. and Lee, P.K.K. 1992. The theory and practice of vacuum preloading. *Computers and Geotechnics*, Vol. 13, pp. 103-118.
- Richart F.E. 1957. A review of the theories for sand drains. *Journal of the Soil Mechanics and Foundations Division, ASCE*, Vol. 83(3), pp. 1-38.
- Rixner, J.J., Kraemer, S.R. and Smith, A.D. 1986 *Prefabricated Vertical Drains*, Vol. I, II and III: Summary of Research Report-Final Report. Federal Highway Admin., Report No. FHWA-RD-86/169, Washington D.C, 433 p.

- Roscoe, K.H., and Burland, J.B. 1968. On the generalized stress strain behavior of wet clay. *Engineering plasticity*, Cambridge Univ. Press; Cambridge, U.K., 535-609.
- Sathananthan, I. 2005. Modelling of Vertical Drains with Smear Installed in Soft Clay. PhD Thesis, Universtiy of Wollongong, 264p.
- Sathananthan, I. and Indraratna, B. 2006. Plane Strain Lateral Consolidation with Non-Darcian Flow. *Canadian Geotechnical Journal*, Vol. 43, pp. 119-133.
- Sathananthan, I. and Indraratna, B. 2006. Laboratory Evaluation of Smear Zone and Correlation between Permeability and Moisture Content. Submitted to *Journal of Geotechnical and Geoenvironmental Engineering*, ASCE (in press).
- Skempton, A.W. 1944. Notes on compressibility of clays. *Quarterly Journal of Geological Society*, London, Vol. 100, No. 2, pp. 119-135.
- Tavenas, P., Jean, P., L eblond, P., and Leroueil, S. 1983. The permeability of natural soft clays. Part II: permeability characteristics. *Canadian Geotechnical Journal*. Vol. 20, pp.645-659.
- Wattegama, C. 2005. The seven tsunamis that hit the isle of Sri Lanka. *Engineering News*, Institution of Engineers Sri Lanka, Vol. 40, No. 3, pp. 6-7.
- Yan, S.W. and Chu, J. 2003. Soil improvement for a road using a vacuum preloading method. *Ground Improvement*, Vol.7, No.4, pp. 165-172.